# Use of ultra-high performance liquid chromatography-high-resolution mass spectroscopy to profile the metabolites from the serum of patients with breast cancer

QINQIN ZHANG[1,2*], RONGZHAO LU[1*], YING WU[3], YONG HONG[2],
NINGXIA WANG[1]  and  CUNCHUAN WANG[4]

[1]Department of Breast Surgery, The First Affiliated Hospital of Jinan University, Guangzhou, Guangdong 510630;
[2]Department of Thyroid and Breast Surgery, Nanxishan Hospital of Guangxi Zhuang Autonomous Region,
Guilin, Guangxi Zhuang Autonomous Region 541002; [3]School of Clinical Medicine, Guilin Medical University,
Guilin, Guangxi Zhuang Autonomous Region 541001; [4]Department of Gastrointestinal Surgery,
The First Affiliated Hospital of Jinan University, Guangzhou, Guangdong 510630, P.R. China

**Abstract.** Breast cancer (BC) is the most common type of malignancy and the leading cause of cancer-associated mortality in women worldwide. As such, assessing the metabolic changes during human breast carcinogenesis is key for developing disease prevention methods and treatment. In the present study, non-targeted metabolomics with chemometrics based on ultra-high performance liquid chromatography-high-resolution mass spectrometry were performed to assess differences in serum metabolite patterns between patients with BC and healthy individuals. A total of 3,246 metabolites in the sera of healthy controls and patients with BC were found. Kyoto Encyclopedia of Genes and Genomes pathway analysis demonstrated that arginine, proline, nicotinate, nicotinamide, caffeine and arachidonic acid metabolism, as well as fatty acid biosynthesis were significantly altered in patients with BC in comparison with controls. These results suggested that serum metabolic profiling has potential for discovering molecular biomarkers for the detection of BC. It may also further the understanding of the underlying mechanisms associated with this disease.

## Introduction

Breast cancer (BC) is a class of highly heterogeneous tumors that can jeopardize the health. BC is not only the most common malignancy in female patients but also the leading cause of cancer-associated mortality in the female population worldwide. In 2020, ~2.3 million female patients were newly diagnosed with BC worldwide and it was the cause of ~685,000 deaths. The incidence of BC varies by region, but appears to be increasing (1). In China, BC now has the highest rate among female malignant tumors and the age at which it first appears is decreasing (2). The occurrence and development of BC is affected by numerous factors (3). Although there have been numerous relevant studies, the pathogenesis of BC has not yet been elucidated (4,5). In the late 1920s, Warburg *et al* (6) reported alterations in aerobic glycolysis in cancer cells. Since then, metabolic changes have been reported in patients with cancer, including the metabolism of amino acids and nucleic acids (7,8). Several experts think that cancer is a series of metabolic diseases (9,10). Thus, understanding metabolic changes in the serum of patients with cancer may provide insight into the biology of cancer. This is beneficial for cancer intervention, and the prevention of metastasis and development of malignant tumors (11).

Metabolomics is a technology that measures the qualitative and quantitative changes of metabolites after a biological system has been subjected to exogenous stimuli (12,13). The occurrence and progression of BC are associated with alteration of metabolites, and metabolomics can analyze these changes that occur during the development and progression of BC, identifying valuable potential markers (14,15). The metabolomics results are affected by the environment, physiology, drugs and other confounding factors. Metabolic biomarkers have been able to discriminate between BC and normal tissue with high sensitivity and specificity, which

*Correspondence to:* Professor Cunchuan Wang, Department of Gastrointestinal Surgery, The First Affiliated Hospital of Jinan University, 613 West Huangpu Road, Guangzhou, Guangdong 510630, P.R. China
E-mail: twcc@jnu.edu.cn

Professor Ningxia Wang, Department of Breast Surgery, The First Affiliated Hospital of Jinan University, 613 West Huangpu Road, Guangzhou, Guangdong 510630, P.R. China
E-mail: 13316268808@163.com

*Contributed equally

has led to development of novel methods for screening and diagnosing BC (16). For example, previous metabolomics methods, such as nuclear magnetic resonance, isotope ratio mass spectrometry (MS) and gas and liquid chromatography (LC)-MS, have been applied to find characteristic markers of the pathogenesis and progression of BC, and each method has its own advantages and disadvantages (17,18).

In the present study, non-targeted metabolomics with chemometrics based on ultra-high performance (UHP) LC-high-resolution (HR)MS was performed to analyze serum samples of patients with BC and healthy individuals to assess metabolite patterns and elucidate potential biomarkers of BC.

**Materials and methods**

*Participants and ethics.* A total of 27 female patients with BC and 30 healthy female control subjects were recruited between May 2020 and September 2021 from the Department of Thyroid and Breast Surgery at Nanxishan Hospital of Guangxi Zhuang Autonomous Region (Guilin, China) before surgery and/or chemotherapy. Patients with BC were between the ages of 36 and 66 years, and the control subjects were between the ages of 22 and 63 years. There was no significant difference in age between the two groups. The study protocol was approved by the Institutional Review Board of the Clinical Research Ethics Committee of Nanxishan Hospital of Guangxi Zhuang Autonomous Region and written informed consent was obtained from each subject. The inclusion criteria for patient recruitment were as follows: i) Age, >18 years; ii) histologically confirmed BC; iii) no metabolic disease and iv) no previous anticancer treatment. For healthy individuals, the inclusion criteria were no abnormalities in their blood test, physical examination or in any imaging results. Clinical parameters and demographic characteristics of subjects are summarized in Table I. Blood samples were collected in the morning before breakfast. The collected blood was immediately centrifuged at 5,000 x g for 10 min at 4°C and the serum was transferred to a clean tube and stored at -80°C until biochemical testing.

*Metabolite extraction.* The serum was diluted using extraction solution (acetonitrile and methanol at 1:1, an internal standard mixture containing isotopic labeling) and mixed for 30 sec in a low-speed vortex machine. The samples were sonicated for 10 min in an ice water bath and incubated for 1 h at -40°C to precipitate proteins. The sample was then centrifuged at 13,800 x g at 4°C for 15 min and the resulting supernatant was transferred to a clean test tube for analysis. Quality control samples were prepared by mixing equal parts of the supernatant of each sample.

*UHPLC-HRMS analysis.* UHPLC-HRMS analysis was performed using an UHPLC system (Vanquish; Thermo Fisher Scientific, Inc.) with an Acquity UPLC BEH Amide Column (2.1x100.0 mm; 1.7 $\mu$m; Waters Corp.) coupled to an Orbitrap Exploris™ 120 MS machine (Thermo Fisher Scientific, Inc.). The mobile phase comprised 25 mol/l ammonium acetate and 25 ammonium hydroxide in water (pH 9.75; phase A) and acetonitrile (phase B). The auto-sampler temperature was at 4°C and the injection volume was 2 $\mu$l. The MS machine

used was able to acquire MS/MS data in an information-dependent acquisition mode using acquisition software (Xcalibur version 4.0.27; Thermo Fisher Scientific, Inc.), which allowed continuous evaluation of the full-scan MS spectrum obtained. The electrospray ionization (ESI) source conditions were as follows: Sheath gas flow rate, 50 Arb; Aux gas flow rate, 15 Arb; nebulizer pressure, 6 bar; flow rate, 0.3 l/min; capillary temperature, 320°C; full MS resolution, 60,000; MS/MS resolution, 115,000; collision energy, 10/30/60, normalized collisional energy mode; and spray voltage, either 3.8 kV (positive) or -3.4 kV (negative).

*Data preprocessing and annotation.* The raw data were converted to mzXML format using ProteoWizard (version 3.0; https://proteowizard.sourceforge.io/). Peak detection, extraction, alignment and integration of data were performed based on the XCMS method (19). Metabolites were annotated using the MS2 database (version 2.1; BiotreeDB). The cutoff for annotation was set at 0.3. To decrease the impact of detection system errors on the results, a series of preparations and a collation of the original data were performed, included filtering of the outlying and missing values, imputation of the missing values and data normalization.

*Statistical analysis.* SIMCA software (v15.0.2; Sartorius Stedim Data Analytics AB; Sartorius AG) was used for analysis. This included univariate statistical analysis (unpaired t-test), principal component analysis (PCA) and orthogonal projections to latent structures-discriminant analysis (OPLS-DA), and the circular line indicates the 95% confidence interval (Hotelling's T-squared ellipse). PCA demonstrated the distribution of the raw data and the OPLS-DA revealed the contribution of the variables to the differences between the two groups. To refine the analysis, the first PC of the variable importance in projection (VIP) was obtained. VIP >1 were selected to represent the metabolite changes. To compare the impact of tumor staging on the aforementioned metabolites, patients with BC were divided into two groups (stage I/IIA, n=19 vs. stage IIB/IIIA, n=8) due to the small number of patients with tumor-node-metastasis stages IIb and IIIa. Comparison of two independent samples were assessed using Student's t-tests. P<0.05 was considered to indicate a statistically significant difference. The relative average normalized number of identified differential metabolites was visualized using heat maps generated using the MeV package. The corresponding metabolic pathways and metabolite set enrichment analysis were analyzed using Kyoto Encyclopedia of Genes and Genomes (KEGG; genome. jp/kegg/) and MetaboAnalyst 2.0 (metaboanalyst.ca) software packages.

**Results**

*Data management.* The ionization source of the HRMS platform used in the present study was ESI, which has two modes of ionization, a positive ion mode (POS) and a negative ion mode (NEG); their combination in detecting the metabolome can produce higher and more precise detection of metabolite coverage (20). POS and NEG datasets were analyzed separately. The raw data contained seven quality control and 57
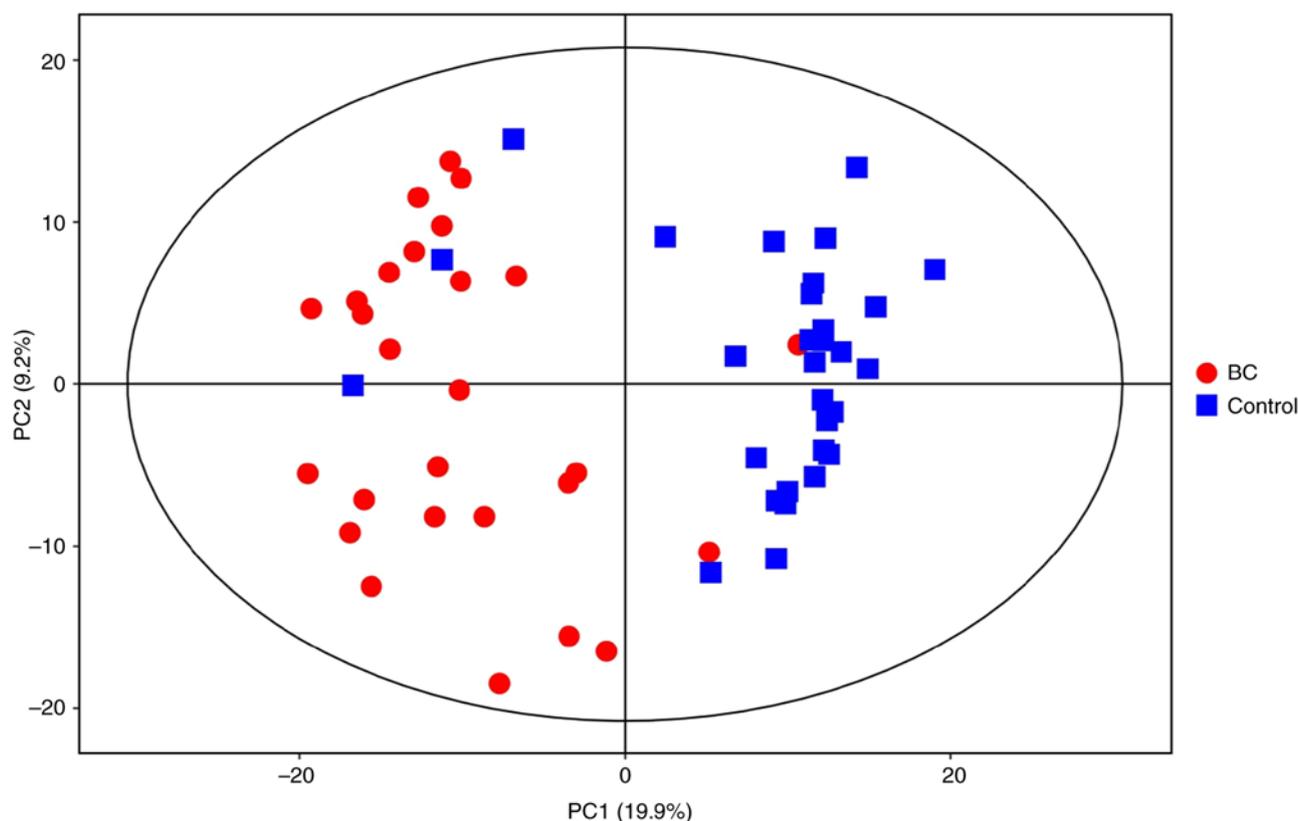
Figure 1. Score scatter plot of the PC analysis model for BC vs. Control groups. The horizontal coordinate displays PC1, the score of the first principal component; the vertical coordinate presents PC2, the score of the second PC; 19.9% refers to the variance contribution rate of PC1; 9.2% refers to the variance contribution rate of PC2. PC, principal component; BC, breast cancer.

Table I. Demographic and clinical pathological characteristics of the study population.

| Characteristic | Patients with BC (n=27) | Healthy control subjects (n=30) |
| --- | --- | --- |
| Median age (range), years | 52 (36-66) | 46 (22-63) |
| TNM stage, n (%) | | |
| I | 8 (29.6) | n.a. |
| IIa | 11 (40.7) | n.a. |
| IIb | 4 (14.8) | n.a. |
| IIIa | 4 (14.8) | n.a. |
| IIIb | 0 (0.0) | n.a. |
| IV | 0 (0.0) | n.a. |

BC, breast cancer; TNM, tumor, node, metastasis; n.a., not applicable.

experimental samples, with 9,404 and 8,401 peaks extracted from POS and NEG, respectively. After data preprocessing, 7,287 and 6,169 peaks were retained from POS and NEG, respectively.

*PCA.* PCA was performed to generate an overview of the variations between the BC and healthy control groups (Fig. 1). Each scatter point represents a sample, and the color and shape of the scatter points represent different groups. A narrower sample point distribution indicates a more similar type and content of metabolites in the sample, while wider sample point distributions indicate larger differences in the overall metabolic level. All samples were within the 95% confidence interval.

*Orthogonal projection to latent structures discriminant analysis.* As an unmonitored PCA model was unable to identify differential metabolites in the serum samples, further discriminant analysis was necessary. To optimize separation between the two groups, OPLS-DA was used to distinguish the metabolic differences. Good discrimination between the two groups was achieved using an OPLS-DA scores plot (Fig. 2), R2X, R2Y and Q2Y were calculated, which varied from 0 to 1. R2X and R2Y represent the fraction of the variance of the x and y variable explained by the model, while Q2Y indicates the predictive performance of the model. The predictive ability of the model was measured by internal validation (POS-models: R2X=0.224, R2Y=0.878 and Q2=0.685; NEG-models: R2X=0.178, R2Y=0.907 and Q2=0.662), suggesting that the model possessed a satisfactory fit with good predictive power. The results of the OPLS-DA score plot (Fig. 2) indicate that the two groups of samples are significantly distinguishable, with all samples falling within the 95% confidence interval.

*Differential metabolite screening and volcano plot for BC vs. healthy control group.* POS qualitatively assigned a total of 1,680 differential metabolites, 120 of which were known. The NEG models collectively identified 1,566 differential
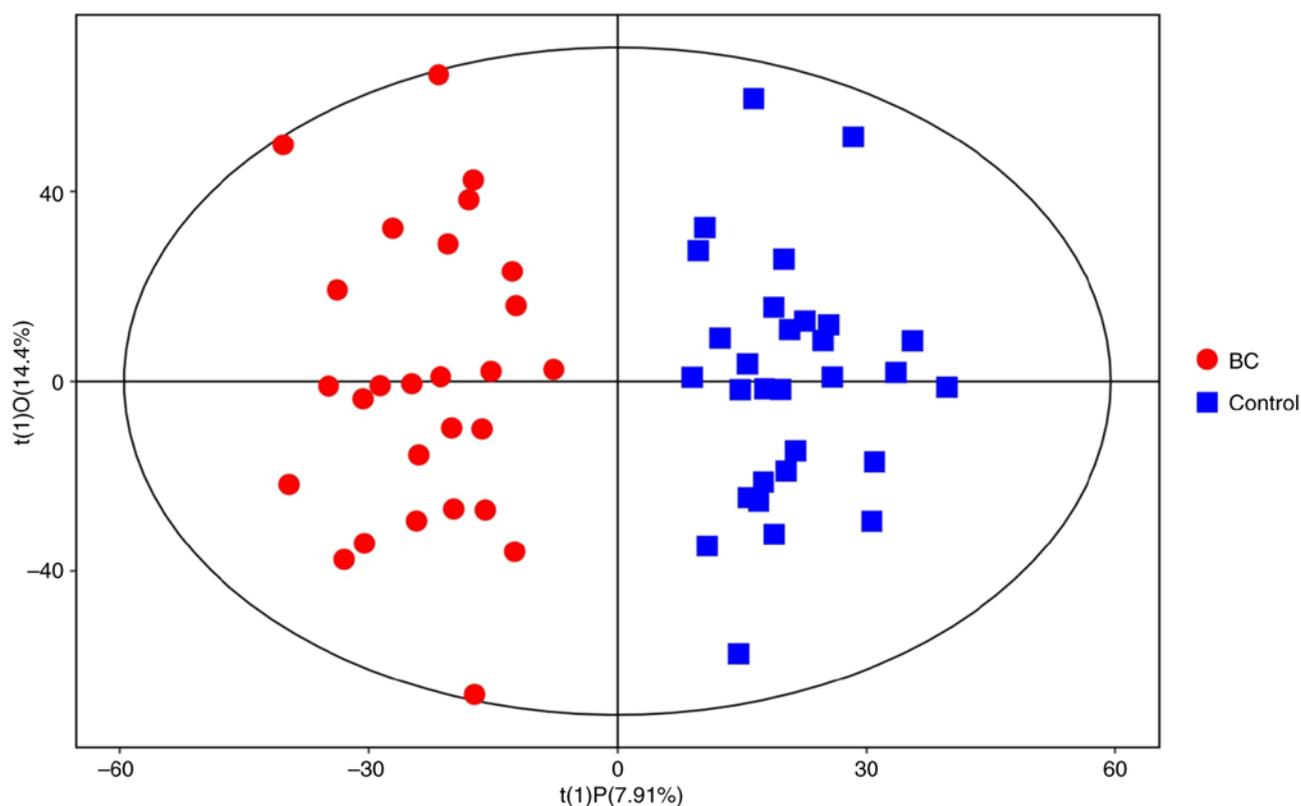
Figure 2. Score scatter plot of orthogonal projections to latent structures-discriminant analysis model for BC vs. Control. The horizontal coordinate t(1)P depicts the predicted PC score of the first principal component; the vertical coordinate t(1)O displays the orthogonal PC score; 7.91% refers to the interpretation rate of the data set by t(1)P; 14.4% refers to the interpretation rate of the data set by t(1)O. BC, breast cancer; PC, principal component.

metabolites, 52 of which were known. There were 2,938 down- and 308 upregulated metabolites in the BC compared with the healthy control group. The results comparing the BC group with the Control group are depicted in the volcano plot (Fig. 3). The findings are presented in two modes: The positive ion mode (Fig. 3A) and the negative ion mode (Fig. 3B). Each point in the volcano plot represents one metabolite and each plot consisted of all the substances measured in the present experiment. The abscissa represents the fold change of the group against each substance, the ordinate represents the P-value of the Student's t-test and the scatter size represents the VIP value of the OPLS-DA model. A larger scatter indicates a greater VIP value obtained. An example of differential metabolite screening results is shown in Table II; the top 10 results are shown for POS and NEG.

The short- and medium-chain fatty acids, including 5Z-dodecenoic acid, 9-decenoic acid, capric acid and myristic acid were significantly decreased in patients with BC compared to normal individuals (fold change, 0.531, 0.516, 0.562 and 0.797, respectively; all P<0.05).

Volcano plots were generated to provide a visual representation of overall distribution of metabolite differences between the groups (Fig. 3). Each point in the volcano plot represents one metabolite and each plot consisted of all the substances measured in the present experiment. The abscissa represents the fold change of the group against each substance, the ordinate represents the P-value of the Student's t-test and the scatter size represents the VIP value of the OPLS-DA model. The larger the scatter, the greater the VIP value obtained.

*KEGG analysis of differential metabolites*. KEGG and MetaboAnalyst were used for pathway enrichment analysis. The metabolic pathways involving the identified metabolites were analyzed and only those with raw P<0.05 were considered to be differential metabolic pathways. The primary metabolic pathways that differed between the control and BC groups were involved in amino acid metabolism, including those associated with arginine and proline (Table III). The other pathways were involved in nicotinate, nicotinamide, caffeine and arachidonic acid (AA) metabolism, as well as fatty acid biosynthesis. The results of the metabolic pathway analysis are presented as bubble plots in Fig. 4. Each bubble in the plot represents a metabolic pathway, and the abscissa and the bubble size represent the effect factor size of that pathway in the topology analysis. The larger the effect factor, the larger the bubble size.

**Discussion**

Cancer is a metabolic disease and carcinogenic cells consume more nutrients and energy than normal cells to support the rapid growth of tumors. This leads to alterations in metabolite levels in the body (21-23). In past decades, there has been a great deal of research into the relationship between tumors and metabolism and these studies may provide a potential approach to identifying novel biomarkers for BC (24,25).

An advantage of metabolomic analysis is the ability to use blood samples. This provides a simple method to obtain metabolic information regarding tumors without need for invasive
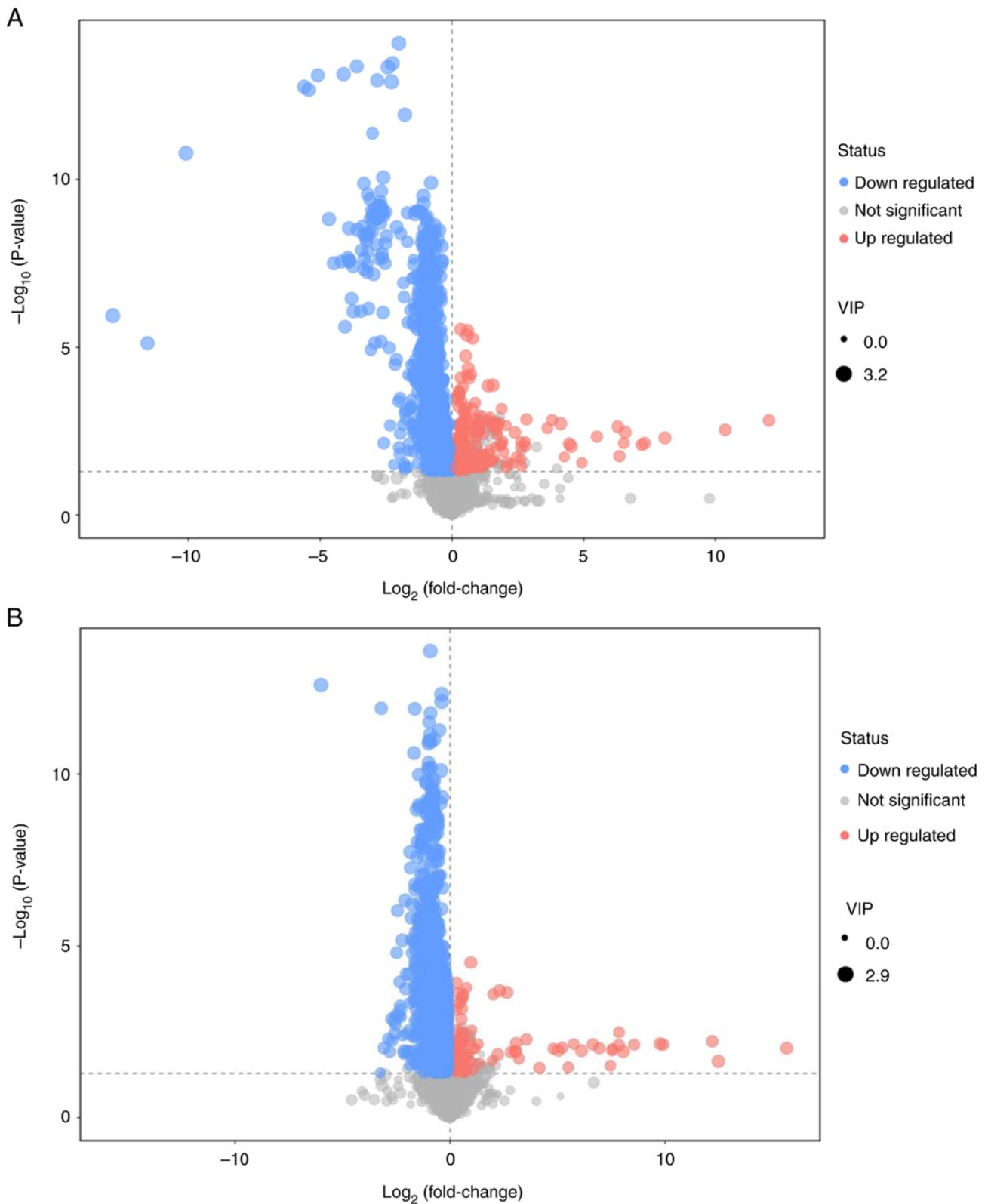
Figure 3. Volcano plot using (A) positive and (B) negative ion mode models. Each point in the volcano plot represents one metabolite and each plot consists of all the substances measured in the present experiment. The abscissa represents the fold change of the group against each substance, the ordinate represents the P-value of the Student's t-test and the scatter size represents the VIP value of the OPLS-DA model. A larger scatter indicates a greater VIP value obtained. BC, breast cancer; VIP, variable importance in projection.

and potentially dangerous biopsies. All factors that affect health of the organism can be reflected in the metabolome. For example, genes, environmental factors, nutrition, drugs, xenobiotics and age lead to changes in the metabolome (26). Hence, metabolomics is expected to serve an important role in elucidating characteristic BC markers.

Table II. Top 10 differential metabolites screened for the positive and negative ion modes.

A, Positive ion mode

| Differential metabolite | VIP | P-value | Fold change | Trend (BC vs. CON) |
|---|---|---|---|---|
| Myo-inositol hexakisphosphate | 1.514 | <0.001 | 0.471 | ↓ |
| 1-pyrroline | 1.391 | 0.023 | 0.771 | ↓ |
| Trigonelline | 1.143 | 0.037 | 0.599 | ↓ |
| Niacinamide | 1.208 | 0.027 | 0.717 | ↓ |
| 6,7-dihydro-5-methyl-5H-cyclopenta[b]pyrazine | 1.836 | 0.003 | 1,320.776 | ↑ |
| Butyramide | 2.473 | <0.001 | 0.564 | ↓ |
| N-methyl-a-aminoisobutyric acid | 1.133 | 0.007 | 0.854 | ↓ |
| 5-aminopentanoic acid | 1.293 | 0.004 | 0.844 | ↓ |
| 1-Methylhypoxanthine | 1.348 | 0.006 | 1.341 | ↑ |
| Ustiloxin D | 1.321 | 0.018 | 0.847 | ↓ |

B, Negative ion mode

| Differential metabolite | VIP | P-value | Fold change | Trend (BC vs. CON) |
|---|---|---|---|---|
| 5Z-dodecenoic acid | 1.996 | <0.001 | 0.531 | ↓ |
| Undecylenic acid | 1.971 | 0.007 | 0.583 | ↓ |
| 3-methyl-2-oxovaleric acid | 1.395 | 0.006 | 0.817 | ↓ |
| 9-decenoic acid | 2.041 | <0.001 | 0.516 | ↓ |
| Capric acid | 1.501 | 0.008 | 0.646 | ↓ |
| Pyrocatechol | 2.305 | 0.000 | 0.309 | ↓ |
| Dodecanoic acid | 1.99 | 0.000 | 0.555 | ↓ |
| Myristic acid | 1.161 | 0.032 | 0.797 | ↓ |
| α-ketoisovaleric acid | 1.161 | 0.024 | 0.877 | ↓ |
| Indoxyl sulfate | 1.923 | <0.001 | 0.442 | ↓ |

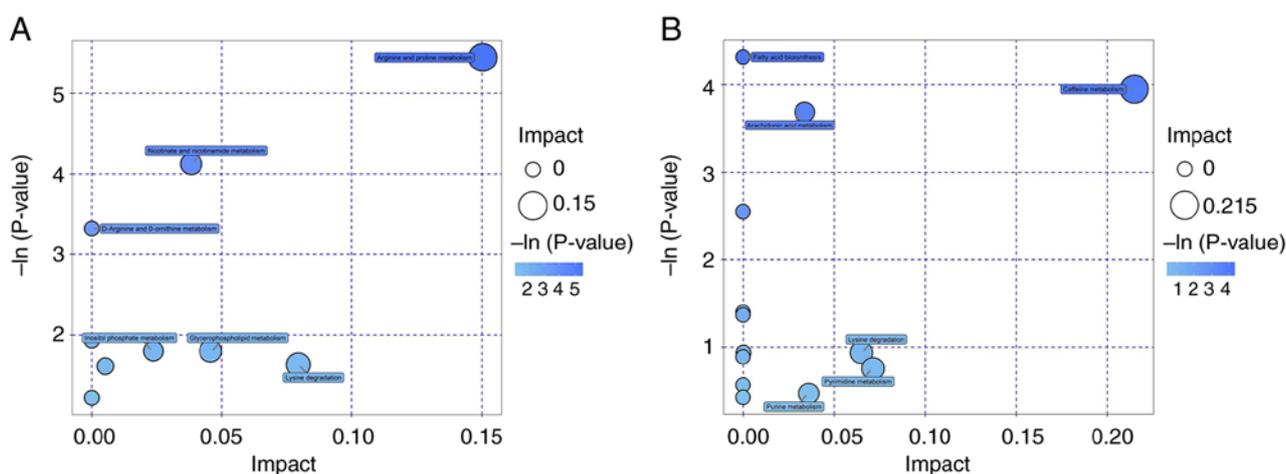VIP, variable importance in projection; BC, breast cancer; CON, control.



Figure 4. Pathway analysis using (A) positive and (B) negative ion mode models. BC, breast cancer.

Rapid proliferation of tumor cells requires large amounts of nutrients, including glucose, lipids and amino acids, to sustain protein synthesis and energy supply. In the present study, blood samples were analyzed by UHPLC-HRMS and metabolites were quantified. A total of 3,246 metabolites were detected in the sera of healthy control individuals and patients with cancer. Among them, 172 could be identified and were classified in different metabolic pathways. Sera from patients

Table III. Metabolic pathways associated with metabolites.

A, Positive ion mode

| Pathway | Hits compound | Cpd |
|---|---|---|
| Arginine and proline metabolism | L-arginine | C00062 |
| | Guanidoacetic acid | C00581 |
| | 5-aminopentanoic acid | C00431 |
| Nicotinate and nicotinamide metabolism | Niacinamide | C00153 |
| | Trigonelline | C01004 |
| D-Arginine and D-ornithine metabolism | L-arginine | C00062 |
| Methane metabolism | Trimethylamine N-oxide | C01104 |
| Inositol phosphate metabolism | Myo-inositol hexakisphosphate | C01204 |
| Glycerophospholipid metabolism | Phosphorylcholine | C00588 |
| Lysine degradation | 5-aminopentanoic acid | C00431 |
| Glycine, serine and threonine metabolism | Guanidoacetic acid | C00581 |
| Aminoacyl-tRNA biosynthesis | L-Arginine | C00062 |

B, Negative ion mode

| Pathway | Hits compound | Cpd |
|---|---|---|
| Fatty acid biosynthesis | Myristic acid | C06424 |
| | Dodecanoic acid | C02679 |
| | Capric acid | C01571 |
| Caffeine metabolism | Caffeine | C07481 |
| | Xanthine | C00385 |
| Arachidonic acid metabolism | Prostaglandin D2 | C00696 |
| | 5,6-DHET | C14772 |
| | 8,9-DiHETrE | C14773 |
| Phenylalanine metabolism | Phenylacetylglycine | C05598 |
| | N-acetyl-L-phenylalanine | C03519 |
| Phenylalanine, tyrosine and tryptophan biosynthesis | Protocatechuic acid | C00230 |
| Pantothenate and CoA biosynthesis | Uracil | C00106 |
| β-alanine metabolism | Uracil | C00106 |
| Primary bile acid biosynthesis | Chenodeoxycholic acid | C02528 |
| Lysine degradation | Glutaric acid | C00489 |
| Fatty acid metabolism | Glutaric acid | C00489 |
| Pyrimidine metabolism | Uracil | C00106 |
| Tryptophan metabolism | Acetyl-N-formyl-5-methoxykynurenamine | C05642 |
| Purine metabolism | Xanthine | C00385 |
| Steroid hormone biosynthesis | Cholesterol sulfate | C18043 |

Cpd, KEGG compound ID; tRNA, transfer RNA; 5,6-DHET, 5,6-dihydroxy-8Z,11Z,14Z-eicosatrienoic acid; 8,9-DiHETrE, 8,9-dihydroxy-5Z,11Z,14Z-eicosatrienoic acid; CoA, coenzyme A.

with BC demonstrated significant alterations in arginine and proline metabolism pathways compared with the healthy controls. There were also significant decreases in L-arginine, guanidoacetic acid and 5-aminopentanoic acid levels.

Arginine is obtained via two key pathways, intracellular endogenous synthesis of arginine primarily from enterocytes and kidneys and extracellular arginine primarily derived from daily food intake (27). However, the endogenous production of intracellular arginine is mainly maintained by *de novo* synthesis from citrulline, using argininosuccinate synthetase 1 (ASS1), which is a rate limiting enzyme. ASS1 gene deletion in tumors results in arginine deficiency, as tumor cells lose the ability to synthesize arginine and as such rely on external sources to support rapid growth with minimal energy expenditure (28). Arginine-deficient tumors include hepatocellular carcinoma, melanoma, malignant pleural mesothelioma and prostate and kidney cancer (29). A previous study also reported that ASS1 deficiency or low expression is common

in tumor cells (30). Notably, higher levels of arginine have been reported in breast tissue from patients with BC compared with benign tissue but lower levels of arginine are observed in the blood (31-33). The present study demonstrated similar results, with significantly lower serum arginine concentrations in patients with BC. Considering the changes in arginine and downstream molecules, the results indicate that the arginine and proline metabolic pathways are altered in patients with BC, potentially due to low expression of ASS1 in tumor cells, in addition to tumor cell depletion. However the mechanisms leading to these changes require confirmation.

In the present study, pathway enrichment analysis revealed that the BC metabolic signaling pathways were also involved in nicotinic acid, nicotinamide, caffeine and purine metabolic pathways. Nicotinic acid and nicotinamide metabolism are associated with high turnover rates of nicotinamide adenine dinucleotide ($NAD^+$) in cancer cells, reflecting their high proliferation rates and DNA synthesis (34). Altered purine and uric acid metabolism may be due to increased tumor demand for substrates for nucleic acid biosynthesis (35).

In the present study, inflammation-related AA metabolic pathway was also significantly altered in patients with BC. AA is an important fatty acid in the n-6 series of polyunsaturated fatty acids and is necessary for the human body. AA is primarily found in cell membranes as phospholipids and is released as a free acid by phospholipases A2 and C, following which it is transformed into bioactive metabolites. It is associated with the development of tumors (36). AA stimulates transformation of sphingomyelin to ceramide and induces apoptosis, thus inhibiting tumor growth (37). A recent study demonstrated that high rate of AA metabolism may be a biomarker for a good prognosis in patients with BC, providing a potential explanation for the poor effect of cyclooxygenase inhibitors in cancer therapy (38).

Although significant differences in metabolic groups were observed between patients with BC and the healthy control individuals, there were certain limitations to the present study. First, the present study involved retrospective data collection and the sample size for each subgroup was small. Second, all histopathology results were diagnosed by one pathologist, which may have led to bias in the data analysis. Third, metabolism is complex and can vary in response to internal and external factors such as dietary intake, medications and health status. However, fasting blood samples were taken in the morning for all subjects prior to any treatment to decrease bias in the present study.

In conclusion, the present study demonstrated significant differences in the metabolites in blood samples obtained from patients with BC and healthy controls. The changes in metabolomic profiles of patients with BC may affect disease biology. However, to the best of our knowledge, the mechanisms leading to these changes are currently unknown. The present study highlighted the usefulness of metabolomics performed on human serum samples obtained from patients with BC. In addition, the present study may provide novel diagnostic and/or prognostic biomarkers to monitor disease progression and treatment.

## Acknowledgements

## Funding

## Availability of data and materials

The data generated in the present study may be found in the Chinese National GeneBank under accession no. CNP0005298 or at the following URL: https://db.cngb.org/search/project/CNP0005298/, DOI: 10.26036/CNP0005298.

## Authors' contributions

CW, RL and YW designed and performed experiments and collected the serum samples from the patients. YW and YH analyzed and curated data, processed images and checked the reliability of the data. QZ analysed and interpreted the data. QZ and NW wrote the original draft, and reviewed and edited the manuscript. NW and CW gave final approval of the version to be published. NW contributed to experimental design and data acquisition. QZ and YH confirm the authenticity of all the raw data. All authors have read and approved the final manuscript.

## Ethics approval and consent to participate

The present study was approved by the Institutional Review Board of the Clinical Research Ethics Committee of Nanxishan Hospital of Guangxi Zhuang Autonomous Region (Guilin, China; approval no. 2019NXSYYEC-003) and each patient provided written informed consent for participation.

## Patient consent for publication

Not applicable.

## Competing interests

The authors declare that they have no competing interests.

## References

1. Arnold M, Morgan E, Rumgay H, Mafra A, Singh D, Laversanne M, Vignat J, Gralow JR, Cardoso F, Siesling S and Soerjomataram I: Current and future burden of breast cancer: Global statistics for 2020 and 2040. Breast 66: 15-23, 2022.
2. Sung H, Ferlay J, Siegel RL, Laversanne M, Soerjomataram I, Jemal A and Bray F: Global cancer statistics 2020: GLOBOCAN estimates of incidence and mortality worldwide for 36 cancers in 185 countries. CA Cancer J Clin 71: 209-249, 2021.
3. Fakhri N, Chad MA, Lahkim M, Houari A, Dehbi H, Belmouden A and El Kadmiri N: Risk factors for breast cancer in women: An update review. Med Oncol 39: 197, 2022.
4. Derakhshan F and Reis-Filho JS: Pathogenesis of triple-negative breast cancer. Annu Rev Pathol 17: 181-204, 2022.
5. Wong GL, Manore SG, Doheny DL and Lo HW: STAT family of transcription factors in breast cancer: Pathogenesis and therapeutic opportunities and challenges. Semin Cancer Biol 86: 84-106, 2022.
6. Warburg O, Wind F and Negelein E: The metabolism of tumors in the body. J Gen Physiol 8: 519-530, 1927.

7. Li S, Zeng H, Fan J, Wang F, Xu C, Li Y, Tu J, Nephew KP and Long X: Glutamine metabolism in breast cancer and possible therapeutic targets. Biochem Pharmacol 210: 115464, 2023.
8. Hamam R, Hamam D, Alsaleh KA, Kassem M, Zaher W, Alfayez M, Aldahmash A and Alajez NM: Circulating microRNAs in breast cancer: Novel diagnostic and prognostic biomarkers. Cell Death Dis 8: e3045, 2017.
9. Gyamfi J, Kim J and Choi J: Cancer as a metabolic disorder. Int J Mol Sci 23: 1155, 2022.
10. Ling ZN, Jiang YF, Ru JN, Lu JH, Ding B and Wu J: Amino acid metabolism in health and disease. Signal Transduct Target Ther 8: 345, 2023.
11. Hanahan D and Weinberg RA: Hallmarks of cancer: The next generation. Cell 144: 646-674, 2011.
12. Guan Q, Liang S, Wang Z, Yang Y and Wang S: $^1$H NMR-based metabonomic analysis of the effect of optimized rhubarb aglycone on the plasma and urine metabolic fingerprints of focal cerebral ischemia-reperfusion rats. J Ethnopharmacol 154: 65-75, 2014.
13. Dudzik D, Barbas-Bernardos C, García A and Barbas C: Quality assurance procedures for mass spectrometry untargeted metabolomics. a review. J Pharm Biomed Anal 147: 149-173, 2018.
14. Huang S, Chong N, Lewis NE, Jia W, Xie G and Garmire LX: Novel personalized pathway-based metabolomics models reveal key metabolic pathways for breast cancer diagnosis. Genome Med 8: 34, 2016.
15. Ogrodzinski MP, Teoh ST and Lunt SY: Metabolomic profiling of mouse mammary tumor-derived cell lines reveals targeted therapy options for cancer subtypes. Cell Oncol (Dordr) 43: 1117-1127, 2020.
16. Araújo R, Bispo D, Helguero LA and Gil AM: Metabolomic studies of breast cancer in murine models: A review. Biochim Biophys Acta Mol Basis Dis 1866: 165713, 2020.
17. Sharma U and Jagannathan NR: Magnetic resonance imaging (MRI) and MR spectroscopic methods in understanding breast cancer biology and metabolism. Metabolites 12: 295, 2022.
18. Choi MH: Mass spectrometry-based metabolic signatures of sex steroids in breast cancer. Mol Cell Endocrinol 466: 81-85, 2018.
19. Huan T, Forsberg EM, Rinehart D, Johnson CH, Ivanisevic J, Benton HP, Fang M, Aisporna A, Hilmers B, Poole FL, et al: Systems biology guided by XCMS Online metabolomics. Nat Methods 14: 461-462, 2017.
20. Yuan M, Breitkopf SB, Yang X and Asara JM: A positive/negative ion-switching, targeted mass spectrometry-based metabolomics platform for bodily fluids, cells, and fresh and fixed tissue. Nat Protoc 7: 872-881, 2012.
21. Griffin JL and Shockcor JP: Metabolic profiles of cancer cells. Nat Rev Cancer 4: 551-561, 2004.
22. Kim YS, Maruvada P and Milner JA: Metabolomics in biomarker discovery: Future uses for cancer prevention. Future Oncol 4: 93-102, 2008.
23. Spratlin JL, Serkova NJ and Eckhardt SG: Clinical applications of metabolomics in oncology: A review. Clin Cancer Res 15: 431-440, 2009.
24. Mishra P and Ambs S: Metabolic signatures of human breast cancer. Mol Cell Oncol 3: e992217, 2015.
25. Johnson CH, Manna SK, Krausz KW, Bonzo JA, Divelbiss RD, Hollingshead MG and Gonzalez FJ: Global metabolomics reveals urinary biomarkers of breast cancer in a mcf-7 xenograft mouse model. Metabolites 3: 658-672, 2013.
26. Johnson CH, Patterson AD, Idle JR and Gonzalez FJ: Xenobiotic metabolomics: Major impact on the metabolome. Annu Rev Pharmacol Toxicol 52: 37-56, 2012.
27. Szefel J, Danielak A and Kruszewski WJ: Metabolic pathways of L-arginine and therapeutic consequences in tumors. Adv Med Sci 64: 104-110, 2019.
28. Hu L, Gao Y, Cao Y, Zhang Y, Xu M, Wang Y, Jing Y, Guo S, Jing F, Hu X and Zhu Z: Identification of arginine and its 'Downstream' molecules as potential markers of breast cancer. IUBMB Life 68: 817-822, 2016.
29. Kim S, Lee M, Song Y, Lee SY, Choi I, Park IS, Kim J, Kim JS, Kim KM and Seo HR: Argininosuccinate synthase 1 suppresses tumor progression through activation of PERK/eIF2α/ATF4/CHOP axis in hepatocellular carcinoma. J Exp Clin Cancer Res 40: 127, 2021.
30. Qiu F, Chen YR, Liu X, Chu CY, Shen LJ, Xu J, Gaur S, Forman HJ, Zhang H, Zheng S, et al: Arginine starvation impairs mitochondrial respiratory function in ASS1-deficient breast cancer cells. Sci Signal 7: ra31, 2014.
31. Park KG, Heys SD, Harris CI, Steele RJ, McNurlan MA, Eremin O and Garlick PJ: Arginine metabolism in benign and malignant disease of breast and colon: Evidence for possible inhibition of tumor-infiltrating macrophages. Nutrition 7: 185-188, 1991.
32. Vissers YL, Dejong CH, Luiking YC, Fearon KC, von Meyenfeldt MF and Deutz NE: Plasma arginine concentrations are reduced in cancer patients: Evidence for arginine deficiency? Am J Clin Nutr 81: 1142-1146, 2005.
33. Geng D, Sun D, Zhang L and Zhang W: The therapy of gefitinib towards breast cancer partially through reversing breast cancer biomarker arginine. Afr Health Sci 15: 594-597, 2015.
34. Navas LE and Carnero A: Nicotinamide adenine dinucleotide (NAD) metabolism as a relevant target in cancer. Cells 11: 2627, 2022.
35. Yin J, Ren W, Huang X, Deng J, Li T and Yin Y: Potential mechanisms connecting purine metabolism and cancer therapy. Front Immunol 9: 1697, 2018.
36. Ortea I, González-Fernández MJ, Ramos-Bueno RP and Guil-Guerrero JL: Proteomics study reveals that docosahexaenoic and arachidonic acids exert different in vitro anticancer activities in colorectal cancer cells. J Agric Food Chem 66: 6003-6012, 2018.
37. Chan TA, Morin PJ, Vogelstein B and Kinzler KW: Mechanisms underlying nonsteroidal antiinflammatory drug-mediatedapoptosis. Proc Natl Acad Sci USA 95: 681-686, 1998.
38. Li W, Guo X, Chen C and Li J: The prognostic value of arachidonic acid metabolism in breast cancer by integrated bioinformatics. Lipids Health Dis 21: 103, 2022.